

Very Heavy Solar Cosmic Rays: Energy Spectrum and Implications for Lunar Erosion

Abstract. *The energy spectrum of solar cosmic-ray particles of the iron group has been determined for the first time over the energy range from 1 to 100 million electron volts per nucleon by the use of glass removed from the Surveyor 3 spacecraft. The difference between the observed (energy)⁻³ spectrum and the limiting spectrum derived previously from tracks in lunar rocks gives an erosion rate of 0 to 2 angstroms per year. High-energy fission of lead, induced by galactic cosmic-ray protons and alpha particles, has also been observed.*

On 19–20 November 1969 Apollo 12 astronauts removed and returned to earth the television camera from the Surveyor 3 spacecraft that had rested on the moon for a period of approximately 2.6 years at a time of maximum solar activity. Housed in the camera, but exposed directly to space, was a clear optical filter in the form of a glass plate highly suitable for the registration of particle tracks. We have used this solid-state nuclear track detector to observe heavy solar nuclei and the effects of other cosmic rays from outside the

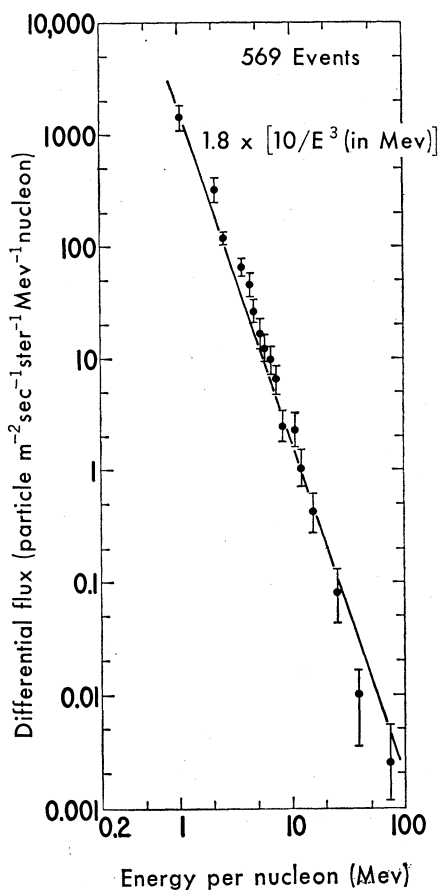


Fig. 1. Differential energy spectrum for iron-group solar cosmic rays. The absolute position along the vertical scale may be in error by approximately 50 percent primarily as a result of uncertainties in the solid angle factor and in the etchable range of an iron track (measured as 0.5 and 28 μm , respectively).

solar system. From the number of nuclei stopping as a function of depth in the detector we have measured the energy spectrum of the solar particles. The difference between the track density versus depth relation we find in the Surveyor glass and the corresponding relations in earlier lunar samples allows us to infer the rate at which erosion exposes new rock surface on the moon. Although the data we present can be further refined in order to yield more extensive and precise information, certain of the results are sufficiently clear and useful to justify this report.

Glass as a detector material (1, 2) has the merit for this work that it does not respond to lightly ionizing particles. This high detection threshold together with what is known of solar abundances (3) ensures that more than 90 percent of the solar particles that are observed will be the iron group nuclei Cr, Mn, Fe, Co, and Ni. Therefore, if from the energy spectrum it is clear that solar particles are present, it is also clear that they are predominantly particles of the iron group.

The filter glass used was a flint glass 3 mm thick of density 3.60 g cm^{-3} and index of refraction 1.612 ± 0.002 , having detection properties somewhat similar to those of the tektite glass reported in (2). The temperature near the glass, just behind the mirror, never exceeded 82°C . For comparison, less than 8 percent fading of ^{252}Cf fission tracks is observed after 1 hour at 125°C ; this result gives considerable confidence that fading of similar tracks at the moon was negligible. The minimum cone angle for ^{252}Cf fission fragments is 30° with an average etchable range of 11 μm ; ^{20}Ne nuclei from a heavy ion irradiation were just detectable, whereas ^{16}O nuclei were not. We estimate, by comparison with earlier calibrations (4), that the minimum cone angle for an iron nucleus is 30° to 35° with an etchable range of 20 to 25 μm . By measuring individual tracks we find cone angles ranging from 35° to 75° and an etchable length of 28 μm for the most abundant tracks,

which we assume to be due to the Fe nuclei. Occasional tracks of length up to 55 μm indicate the presence of nuclei heavier than iron in less than 15 percent abundance. The cone angle is of great importance since it equals the minimum angle of inclination to a surface at which a track is etched (1, 2) and hence determines the solid angle through which tracks of incident particles are revealed by etching. The specific geometry of the housing over the filter (5) was such as to shield out particles over most of the upward-facing hemisphere, thus allowing Fe nuclei of energy less than 22 Mev per nucleon entrance only over a solid angle factor estimated to be 1.3 steradians, centered around a line inclined at about 30° to the glass surface. Our measurements of individual tracks show them to be grouped within 23° or 24° of this line. Consequently, we may assume for simplicity that the particles detected arrive as a collimated beam at an angle of incidence of 30° with an effective solid angle factor of 0.5. In order that the particles be observed with maximum efficiency, the glass was cut and polished with a surface normal to this direction. In this

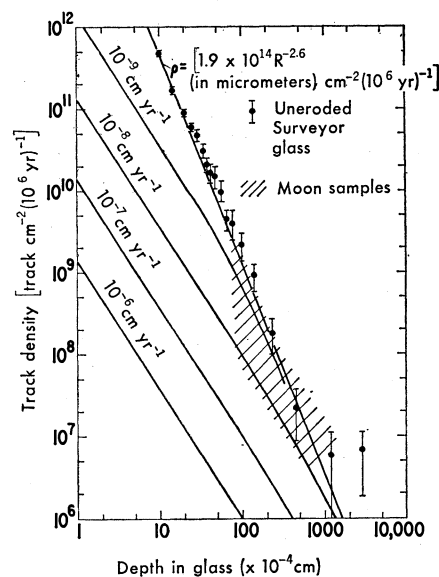


Fig. 2. Effect of erosion on the track gradients as compared with corresponding observations in lunar rocks. An erosion rate of 0 to $2 \times 10^{-8} \text{ cm yr}^{-1}$ is consistent with the track densities observed (10, 13) in lunar samples 10017 and 10003. The track densities and depths of the moon samples have been recalculated for direct comparison with the Surveyor glass by means of a solid angle factor of $\pi/2$, an etchable range of Fe of 10 μm , and an exposure time of 5×10^6 years for one side of the rock. Only observations at depths $>50 \mu\text{m}$ are included. For the Surveyor glass a solid angle factor of 0.5 and an etchable range of 28 μm are used.

geometry a particle traveling through the center of the opening in the housing must traverse a distance through the glass equal to $3\frac{1}{2}$ times the distance from its intersection with the polished surface up to the exposed original top surface of the glass. We etched the tracks for 3 minutes with 5.7 percent HF to remove a $7\text{-}\mu\text{m}$ layer from the surface; this procedure revealed a track density versus depth relation that diminishes sharply from $(2.6 \pm 0.2) \times 10^6$ track cm^{-2} at a position corresponding to a depth of 3.6 mg cm^{-2} to 35 ± 20 track cm^{-2} at 700 mg cm^{-2} and beyond (5a).

These results, which are illustrated in Fig. 1, show a flux Φ that is well fitted up to 100 Mev per nucleon by a relation $\Phi = 1.8 \times 10^3 E^{-3}$ particle $\text{m}^{-2} \text{sec}^{-1} \text{ster}^{-1} \text{Mev}^{-1}$ nucleon, where E is the energy in million electron volts per nucleon. We deduced the energy from the range, using curves calculated for olivine (6) and corrected (7) for the particular glass composition involved (8). The energies for a given gram per square centimeter of stopping material were reduced by 20 percent, which should be within 5 percent of the true correction (7). The E^{-3} reduction of the spectrum identifies it as solar in origin, since this is the behavior that is often observed for alpha particles from individual solar flares (9), and inferred less directly for nuclei of the iron group over a limited energy range (10). Although our curve gives no clear evidence of curvature, a flattening of the spectrum at still lower energies is likely. At higher energies (greater depths in glass), the track density levels off above 100 Mev per nucleon because of fission events produced by the penetrating background of galactic cosmic-ray protons and alpha particles.

Several particle tracks were of distinctive V-shapes that are characteristic of high energy-induced fission (11) such as has been seen after accelerator irradiations but not previously from cosmic-ray irradiation. Because of the observed uniform distribution with depth at which the fission occurred, this type of track is most likely caused by Pb in the glass fissioning in response to penetrating primary cosmic-ray particles, mostly galactic protons and alpha particles. We can estimate how frequent the formation of recognizable events characterized by a V-shape should be and test this hypothesis by calculating the following six-term product: the proton plus alpha particle fluence over 2.6 years ($2\pi \times 2.5 \times 10^7$ particle cm^{-2}),

the cross section (12) for the fission [$(0.8 \text{ to } 1.2 \times 10^{-25} \text{ cm}^2)$] of lead, the number of lead atoms per volume in the glass (4.4×10^{21} atom cm^{-3}), the etchable range of the fission fragments ($10 \mu\text{m}$), and the etching efficiency (11) for events characterized by a V-shape (0.10 to 0.15). This product gives 10 ± 5 track cm^{-2} as the expected track density. We observed eight definite V-shaped tracks in 0.50 cm^2 or 16 ± 6 track cm^{-2} in agreement with the calculated number.

The energy spectrum in Fig. 1 is a key to measuring erosion on the moon. The shaded band in Fig. 2 shows the track densities versus depth measured by four groups (10, 13) in lunar samples 10017 and 10003. For moon rocks the exposures to low-energy cosmic rays occur typically over many millions of years (10, 13), so that there is ample time for erosional processes to wear away surfaces. For such a situation, points at a final depth R in the rock have accumulated tracks when the actual depth ranged from R to $(R + vt)$, where v is the rate of erosion and t is the time over which the sample served as a detector of heavy cosmic rays. If the erosion is uniform on a scale small as compared with vt , and if the range spectrum of cosmic rays is proportional to $R^{-2.6}$ (which Fig. 2 shows to be a good approximation), then the ratio of the observed to the uneroded track density will be

$$\left[1 - \frac{1}{1 + (vt/R)^{1.6}} \right] \left(\frac{R}{1.6vt} \right)$$

Hence, for small R the track density varies as $R^{-1.6}$, with the actual magnitude depending on v , whereas at large R the $R^{-2.6}$ variation occurs. The break from slope 1.6 to slope 2.6 depends on the product vt , so that in principle two measurements along the curve determine both v and t .

In Fig. 2 the track densities observed in two of the most extensively studied Apollo 11 moon samples (10, 13) are compared with those calculated to result from the observed range spectrum if a constant rate of erosion takes place at 10^{-6} , 10^{-7} , 10^{-8} , or 10^{-9} cm yr^{-1} . The fluence observed here for 2.6 years is assumed to constitute half of that of an average 11-year solar cycle. It is clear that a range of values from 0 to 2×10^{-8} cm yr^{-1} is in agreement with the data. Such values are consistent with the upper limits of 10^{-7} cm yr^{-1} set for a number of lunar samples (10, 13) by other lines of reasoning, but are much less than the $\sim 2 \times 10^{-7}$ cm yr^{-1} in-

ferred by Shoemaker *et al.* (14) by extrapolation of observed impact crater frequencies into the unexplored region of small craters. This discrepancy suggests that the micrometeorite flux that is responsible for subcentimeter craters may well be much less than has previously been thought. The observed erosion rate of an atomic layer per year (or per few years) suggests also the possibility that an atomic process may be responsible, rather than a macroscopic cratering phenomenon (15).

Although we infer a low rate of erosion here, it is worth noting that a number of effects could cause greater rates to be derived from track counts in moon samples: statistical fluctuations in the actual erosion due to micrometeorites or secondary ejecta (16), a thin covering layer of dust, or track counts not taken along the steepest track gradient. Nevertheless, our results show that higher erosion rates are by no means universal and that the moon is a somewhat calmer place that was previously thought.

There exists appreciable uncertainty in the long-term average flux of solar particles. If the present solar cycle has furnished fewer track-forming flare particles than the long time average, for example, by a factor of 2, then approximately twice the erosion must have occurred. It should be emphasized that we are also implicitly assuming that our functional relation of (energy) $^{-3}$ observed over 2.6 years of solar activity is an adequate representation over many millions of years, an assumption we cannot at present establish with certainty (17).

R. L. FLEISCHER
H. R. HART, JR.
G. M. COMSTOCK

General Electric Research and
Development Center,
Schenectady, New York 12301

References and Notes

1. R. L. Fleischer and P. B. Price, *J. Appl. Phys.* **34**, 2903 (1963); —, R. M. Walker, *Annu. Rev. Nucl. Sci.* **15**, 1 (1965).
2. R. L. Fleischer, P. B. Price, R. T. Woods, *Phys. Rev.* **188**, 563 (1969).
3. L. H. Aller, *Abundance of the Elements* (Wiley, New York, 1961).
4. P. B. Price, R. L. Fleischer, C. D. Moke, *Phys. Rev.* **167**, 277 (1968).
5. "Surveyor III Program Results," *Nat. Aeronaut. Space Admin. Spec. Publ. SP-184* (1969).
- 5a. Since this report was submitted for publication, N. Nickle (unpublished proceedings of the 2nd Lunar Science Conference, Houston, 11-14 January 1971) has noted that a dust covering was present on the filter during its exposure on the moon. From measurements on the returned filter (J. Rennilson and D. Robertson, unpublished observations), we infer the thickness of this cover to be 0.3 to 1.5 mg cm^{-2} . Although such a layer would not alter our inferred spectrum appreciably, it could distort results for energies below 1 Mev per nucleon.

6. R. P. Henke and E. V. Benton, "Range and Energy Loss Tables" [*U.S. Nav. Radiol. Def. Lab. Tech. Rep. TR-1102* (1966)].
7. L. C. Norcliffe and R. L. Schilling, *Nucl. Data*, in press.
8. From the possible flint glasses [G. W. Morey, *The Properties of Glass* (Reinhold, New York, ed. 2, 1954)] with the known density and index of refraction, a nominal composition (in percentage by weight) of SiO₂, 46; PbO, 46; Na₂O, 4; and K₂O, 4 was inferred to be a good approximation for calculating the energies. Wet chemical analysis has given 43 percent PbO.
9. K. A. Anderson, *Proc. Int. Conf. Cosmic Rays, 11th, Budapest, 1969*, p. 315.
10. R. L. Fleischer, E. L. Haines, H. R. Hart, Jr., R. T. Woods, G. M. Comstock, *Geochim. Cosmochim. Acta* 3 (Suppl 1), 2103 (1970).
11. R. L. Fleischer, C. W. Naeser, P. B. Price, R. M. Walker, M. Maurette, *J. Geophys. Res.* 70, 1491 (1965).
12. N. A. Perfilov, *J. Exp. Theor. Phys.* 14, 623 (1962).
13. G. Crozaz, U. Haack, M. Hair, M. Maurette, R. M. Walker, D. Woolum, *Geochim. Cosmochim. Acta* 3 (Suppl. 1), 2051 (1970); P. B. Price and D. O'Sullivan, *ibid.*, p. 2351; D. Lal, D. Macdougall, L. Wilkening, G. Arrhenius, *ibid.*, p. 2295.
14. E. M. Shoemaker, M. H. Hait, G. A. Swann, D. L. Schleicher, G. G. Shaber, R. L. Sutton, D. H. Dahlem, E. N. Goddard, A. C. Waters, *ibid.*, p. 2399.
15. For example, if one atom of the exposed surface were removed for each incident solar wind ion, it would give the observed erosion rate.
16. A recent flaking off of a 100- μ m chip would leave a surface with a lower track density characteristic of a greater (that is, 100 μ m) depth. Thus, for example, the large discrepancy between the track density profiles of rock 10058 and of rock 10017 or 10003 would be resolved if a 75- to 300- μ m chip had rather recently been removed from rock 10058, either by a natural process or in handling during recovery.
17. However, one test of this assumption will come from repeated evaluation of t from the place of break in the curve from $R^{-1.6}$ to $R^{-2.6}$. If this age consistently agrees with values that are independently derived from the galactic cosmic rays (10, 13), it will constitute strong support for the long time applicability of an E^{-3} relation.
18. We thank E. L. Haines for bringing to our attention the fact that Surveyor 3 parts were to be returned to earth, W. R. Giard and E. Stella for experimental assistance, E. W. Balis, L. B. Bronk, and D. H. Wilkins for prompt chemical analysis of the glass, R. C. DeVries for measuring the index of refraction, and N. Nickle for numerous communications relative to the exposure of the glass. We are indebted to the National Aeronautics and Space Administration for supplying the Surveyor glass.

17 December 1970

-.70, $P < .001$) with sunspot cycle length over the period 527 B.C. to A.D. 1964 (8). The significance of this correlation is that there was a strong relationship ($r = -.64$, $P < .001$) between sunspot cycle length (measured from cycle maximums) and mean yearly sunspot number per cycle for the European data over the interval A.D. 1699 to 1964 (9). The correlation between the solar index and sunspot cycle length is important because of the statements of Schove (6, pp. 127-128) which indicate that he was not using sunspot cycle length as a possible guide to his assessment of sunspot (or auroral) activity. Indirect evidence for the validity of the index is: (i) a correlation ($r = -.51$, $P < .01$) of 31 outlined solar activity periods from 527 B.C. to A.D. 1964 with ¹⁴C variation (8); (ii) a change in ¹⁴C activity inverse to the change in solar activity in 22 of 24 instances for a $X^2 = 20.2$, $P < .001$ (8); and (iii) a negative correlation ($r = -.55$, $P < .05$) of the solar index with ¹⁸O variation for the 17 centuries since A.D. 300 (10).

The period of sunspot dearth from around A.D. 1645 to 1715 was noted to have preceded a period of maximum glacial advance in Alaska, British Columbia, and Oregon (11). Subsequent study (12) found that for the Pacific Northwest, British Columbia, and Alberta, two intervals, 1711 to 1724 and 1835 to 1849, contained over one-half the glacial advances from 1580 to 1900. These intervals followed the two lowest periods of European solar activity measurements (1645 to 1715 and 1798 to 1833). A further analysis (9) found that given a lag period of 18 years to allow for ice accumulation and flow to the terminus, there was a X^2 of 7.7 ($P < .006$) for the hypothesis that an equal number of glacial advances should occur after the four highest and the four lowest sunspot activity periods since 1611.

A summary of worldwide glaciation patterns since the 5th century B.C. (2) found that this activity was historically synchronous throughout the world and that glaciation was associated with periods of lower solar activity if these periods were of sufficient length and were not preceded by long intervals of higher solar activity. The tendency of solar periods of sufficient length to have a climatic impress was demonstrated in a rank correlation ($r =$

Solar-Climate Relationships in the Post-Pleistocene

Abstract. *The most conspicuous climatic aberration of the past two millennia was the temperature decline and glacial advance of the A.D. 1550 to 1900 period. This temperature decline has been correlated with an interval of lower solar activity and there is evidence from both the post-Pleistocene glacial record and from oxygen-18 analysis that such an interval has recurred at cyclic periods of around 2400 to 2600 years.*

During the past several millennia, temperature changes have occurred which have been correlated with variation in solar output, both for the period of European solar observations and for the longer interval of the less exact Oriental observations (1). These correlations have been demonstrated mainly on time intervals of a century or more and are in contrast to the lack of agreement in studies of solar-climate relationships on the scale of a year or less. The greater agreement in solar-climate correlations on a broader time scale is possibly the result of oceanic thermal inertia, but whatever the reason, the correlations reached a higher statistical significance when a cumulative index of solar activity was used (1).

The likelihood of some sort of solar control over climate has been greatly enhanced in the last 2 years by the discovery of cycles of around 2400 to 2600 years in the periodicity of glacial advance (2, 3) and in the temperature-related $\delta^{18}\text{O}$ data from the Greenland Camp Century ice core (4). There is evidence that these cycles are based on

variation in solar activity and they have been used for extrapolation into the recent past and near future. Whether solar cycles of larger temporal amplitude have a climatic influence is still unknown; their potential discovery will be implemented if the nature of solar-climate relationships on smaller scales is better understood.

European measurements of sunspot activity have been summarized (5) from 1610 to 1960 and continued to the present. Of less reliability are the more extensive Oriental observations of sunspot and auroral activity (6, 7) which were erratically recorded by numerous observers over the period 522 B.C. to the present. These data were combined into a single solar index (8), which, by using both sunspot and auroral observations, or either of these if the other were missing, was able to present an index for 206 of the 227 single sunspot cycles since 522 B.C.

The reliability of this solar index has been shown by both internal evidence and by indirect methods. The index was negatively correlated ($r =$